Comparative Analysis of Double Drift Region and Double Avalanche Region IMPATT Diodes

ALEXANDER ZEMLIAK, ROQUE DE LA CRUZ
Department of Physics and Mathematics
Puebla Autonomous University
Av. San Claudio y 18 Sur, Puebla, 72570
MEXICO

Abstract: - The comparative analysis of the well known DDR (Double Drift Region) IMPATT diode structure and the new n^+pvnp^+ structure for the avalanche diode has been realized on the basis of the precise numerical model. The new type of the diode was named as the Double Avalanche Region (DAR) IMPATT diode. This structure includes the two avalanche regions inside the diode. The phase delay, which was produced by means of the two avalanche zones and the drift zone *v* is sufficient for the negative resistance obtain for the wide frequency region. The numerical model that is used for the analysis of the various diode structures includes all the principal features of the physical phenomena inside the semiconductor structure. The admittance characteristics of both types of the diodes were analyzed in very wide frequency region.

Key-Words: - Semiconductor microwave devices, modeling and simulation, numerical methods.

1 Introduction

The problem of the microwave power generation of the sufficient output level is the essential problem of modern semiconductor electronics. The more powerful semiconductor device is the IMPATT diode of the different structures. The single drift region (SDR) and the double drift region (DDR) IMPATT diodes are very well known [1-3] and are used successfully for the microwave power generation in millimeter region. The simulation and optimization of its parameters [4-9] can obtain very high output power level and serves as the basis for the technology to produce the diodes with the extremely characteristics. From the beginning [10] the main idea to obtain the negative resistance was defined on the basis of the phase difference producing between RF voltage and RF current due to the delay in the avalanche build-up process and the transit time of charge carriers. The transit time delay of both types of the diodes is the essential factor of the necessary phase conditions fulfillment to obtain the negative resistance. However a diode that has two avalanche regions can produce an avalanche delay, which alone can satisfy the necessary conditions to generate the microwave power. In this case the phase delay of the drift zone becomes subsidiary. The DDR diode and the DAR diode can be defined by means of the next two structures (n+npp+, n+p*v*np+) in Fig. 1 (a), (b).

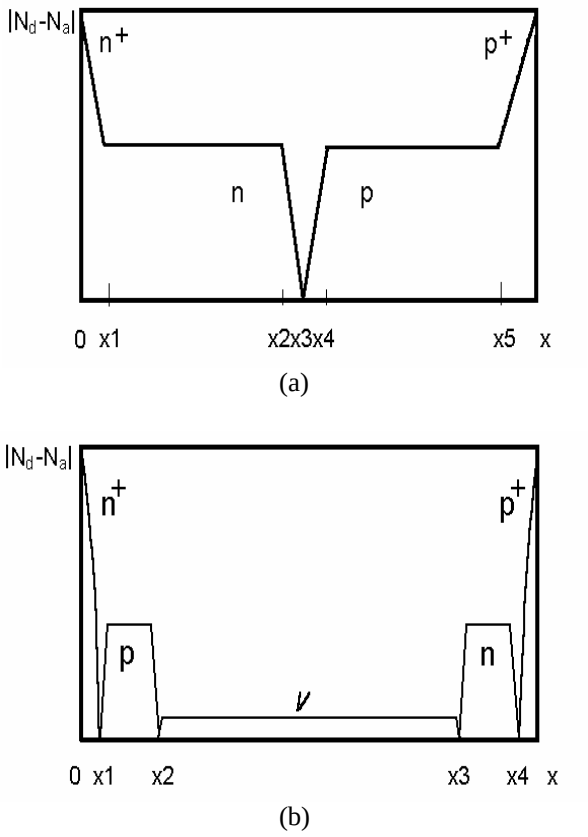

Fig. 1. Doping profile of DDR - (a) and DAR - (b) IMPATT diode.

The DAR diode has two avalanche regions around n+p and np+ junctions and one common drift region. This type of diode was suggested in [11]. The characteristics of this diode type were analyzed in DC and RF modes [12-15]. Each of the avalanche zones provides the phase delay about p and this is sufficiently to produce the negative diode resistance. The electric field distribution along the axis x for both types of the diodes can be approximate by the Fig. 2.

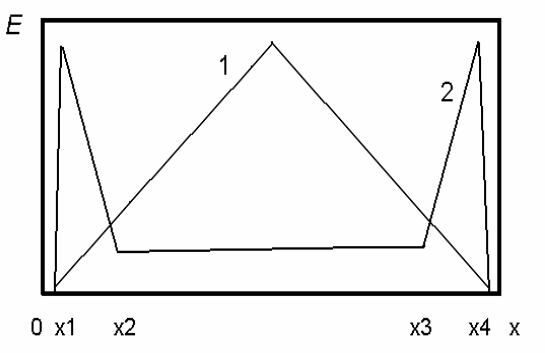

Fig. 2. Electric field distribution for DDR - 1 and DAR - 2 IMPATT diode

There is one avalanche zone for DDR diode and two avalanche zones for DAR diode. The authors of the works [11-15] affirm that the drift zone transit time delay is not a critical parameter for DAR diode because of the total avalanche delay equal to p. Some advantages of the DAR structure were prognoses due this fact. The analysis provided in [11-15] gave the interesting and, at the same time very surprised results concerning the main features of the DAR diodes. Some of these results were obtained by means of the small signal model [11-13]. Others results [14-15] were obtained on the basis of simplified nonlinear model. We suppose that there is a necessity to analyze these structures on the basis of the precise model of the IMPATT diode, which was developed in some works of the authors [16-17].

2 Numerical Model

The electrical model which is useful for the precise analysis of the internal diode structure describes of all important physical phenomena into the semiconductor device. This model is based on the system of two continuity equations for the electrons and holes, the Poisson equation for the potential distribution in semiconductor structure and the necessary boundary conditions as for continuity equations and for the Poisson equation.

The system of the continuity equations include two differential equations for the carriers concentrations and two additional equations for the current density determination:

$$\frac{\partial n(x,t)}{\partial t} = \frac{\partial J_n(x,t)}{\partial x} + \alpha_n \left| J_n(x,t) \right| + \alpha_p \left| J_p(x,t) \right|$$

$$\frac{\partial p(x,t)}{\partial t} = -\frac{\partial J_p(x,t)}{\partial x} + \alpha_n \left| J_n(x,t) \right| + \alpha_p \left| J_p(x,t) \right| \qquad (1)$$

$$J_n(x,t) = n(x,t)\, V_n + D_n \frac{\partial n(x,t)}{\partial x}$$

$$J_p(x,t) = p(x,t)\, V_p - D_p \frac{\partial p(x,t)}{\partial x}$$

where n, p are the concentrations of electrons and holes; J_n, J_p are the current densities; α_n, α_p are the ionization coefficients; V_n, V_p are the drift velocities; D_n, D_p are the diffusion coefficients. Ionization coefficients, drift velocities and diffusion coefficients are the functions of two arguments; the spaces coordinate x and the times coordinate t.

The dependences of the ionization coefficients α_n, α_p on field and temperature have been approximated using the approach described in [18]:

$$\alpha_n(E,T) = \begin{cases} 2.6 \cdot 10^6 \, e^{-\left[\left(1.4 \cdot 10^6 + 1.3 \cdot 10^3 \cdot T\right)/E\right]} & E < 2.4 \cdot 10^5 \\ 6.2 \cdot 10^5 \, e^{-\left[\left(1.05 \cdot 10^6 + 1.3 \cdot 10^3 \cdot T\right)/E\right]} & 2.4 \cdot 10^5 < E < 5.3 \cdot 10^5 \\ 5.0 \cdot 10^5 \, e^{-\left[\left(0.96 \cdot 10^6 + 1.3 \cdot 10^3 \cdot T\right)/E\right]} & E > 5.3 \cdot 10^5 \end{cases} \qquad (2)$$

$$\alpha_p(E,T) = \begin{cases} 2.0 \cdot 10^6 \, e^{-\left[\left(1.95 \cdot 10^6 + 1.1 \cdot 10^3 \cdot T\right)/E\right]} & 2.0 \cdot 10^5 < E < 5.3 \cdot 10^5 \\ 5.6 \cdot 10^5 \, e^{-\left[\left(1.296 \cdot 10^6 + 1.1 \cdot 10^3 \cdot T\right)/E\right]} & E > 5.3 \cdot 10^5 \end{cases}$$

The temperature T is expressed in $^{\circ}C$ and the electrical field E is expressed in *V/cm*. The drift velocities and diffusion coefficients were calculated by means of the approximations have given in [19-21]. These approximations include all of the essential features of the carrier's mobility in silicon semiconductor structure and give the possibility to calculate the diode behavior in a wide frequency region for the different regimes.

The boundary conditions for this system include the concentration and the current definition for contact points and can be written as follows:

$$n(0,t) = N_D(0); \qquad p(l_0,t) = N_A(l_0);$$
$$J_n(l_0,t) = J_{ns}; \qquad J_p(0,t) = J_{ps}. \tag{3}$$

where J_{ns}, J_{ps} are the electron current and the hole current for inversely biased *p-n* junction; $N_D(0)$, $N_A(l_0)$ are the concentrations of donors and acceptors at two end space points x = 0 and x = l_0; where l_0 is the length of the active layer of semiconductor structure.

The electrical field distribution into semiconductor structure can be obtained from Poisson equation. As electron and hole concentrations are functions of the time, therefore, this equation is the time dependent too and time is the equation parameter. Poisson equation for the above defined problem has the following form:

$$\frac{\partial E(x,t)}{\partial x} = -\frac{\partial^2 U(x,t)}{\partial x^2} = N_D(x) - N_A(x) + p(x,t) - n(x,t) \tag{4}$$

where $N_D(x)$, $N_A(x)$ are the concentrations of donors and acceptors accordingly, *U(x,t)* is the potential, *E(x,t)* is the electrical field.

The boundary conditions for this equation are:

$$U(0,t) = 0; \quad U(l_0,t) = U_0 + \sum_{m=1}^{M} U_m \sin\left(w\, mt + j_m\right) \tag{5}$$

where U_0 is the DC voltage on diode contacts; U_m is the amplitude of harmonic number *m*; w is the fundamental frequency; j_m is the phase of harmonic number *m*; *M* is quantity of harmonics.

Equations (1) - (4) adequately describe processes in the IMPATT diode in a wide frequency band. However, numerical solution of this system of equations is very difficult because of the existing a sharp dependence of equation coefficients on electric field. Evident numerical schemes have poor stability and require a lot of computing time for good calculation accuracy obtaining. It is more advantageous to use non-evident numerical scheme that has a significant property of absolute stability. Computational efficiency and numerical algorithm accuracy are improved by applying the space and the time coordinates symmetric approximation.

After the approximation of functions and its differentials, the system (1) is transformed to the non-evident modified Crank-Nicholson numerical scheme. This modification consists of two numerical systems, each of them having three-diagonal matrix. This system has the following form:

$$-(a_n - b_n)\, n_{i-1}^{k+1} + (1 + 2a_n)\, n_i^{k+1} - (a_n + b_n)\, n_{i+1}^{k+1} =$$
$$a_n\, n_{i-1}^{k} + (1 - 2a_n)\, n_i^{k} + a_n\, n_{i+1}^{k} + b_n\,(n_{i+1}^{k} - n_{i-1}^{k}) +$$
$$a_n \left| t \cdot V_n \cdot n_i^k + r \cdot D_n \cdot (n_{i+1}^k - n_{i-1}^k) \right| +$$
$$a_p \left| t \cdot V_p \cdot p_i^k - r \cdot D_p \cdot (p_{i+1}^k - p_{i-1}^k) \right| \tag{6}$$

$$-(a_p + b_p)\, p_{i-1}^{k+1} + (1 + 2a_p)\, p_i^{k+1} - (a_p - b_p)\, p_{i+1}^{k+1} =$$
$$a_p\, p_{i-1}^{k} + (1 - 2a_p)\, p_i^{k} + a_p\, p_{i+1}^{k} - b_p\,(p_{i+1}^{k} - p_{i-1}^{k}) +$$
$$a_p \left| t \cdot V_p \cdot p_i^k - r \cdot D_p \cdot (p_{i+1}^k - p_{i-1}^k) \right| +$$
$$a_n \left| t \cdot V_n \cdot n_i^k + r \cdot D_n \cdot (n_{i+1}^k - n_{i-1}^k) \right|$$

i = 1, 2, ... $I_1 - 1$; k = 0, 1, 2, ...∞

where $a_{n,p} = \frac{t\ D_{n,p}}{2h^2}$; $b_{n,p} = \frac{t\ V_{n,p}}{4h}$; $r = \frac{t}{2h}$; i is the space coordinate node number; k is the time coordinate node number; h is the space step; t is the time step; I_1 is the space node number.

The approximation of the Poisson equation is performed using the ordinary finite difference scheme at every time step k:

$$U_{i-1}^k - 2U_i^k + U_{i+1}^k = h^2\left(N_{Di} - N_{Ai} + p_i^k - n_i^k\right) \tag{7}$$

Numerical algorithm for the calculation of IMPATT diode characteristics consists of the following stages: 1) the voltage is calculated at the diode contacts for every time step; 2) the voltage distribution is calculated at every space point from Poisson equation by factorization method [16], the electrical field distribution along the diode active layer is calculated; 3) the charge carries ionization and drift parameters are calculated in numerical net nodes for the current time step; 4) the system of equations (6) is solved by matrix factorization method and electron and hole concentration distributions are calculated for the new time step. After this, the calculation cycle is repeated for all time steps until the end of the time period. This process is continued from one period to another until the convergence is achieved by means of the results comparison for two neighbor periods. Then all harmonics of the external current; admittance for the harmonic number *m* and power characteristics can be found by the Fourier transformation.

3 Numerical Scheme Convergence

The numerical scheme (6)-(7) characteristic analysis for the different DDR IMPATT diode had been made some years ago [16]. This analysis showed a good convergence of the numerical model. The convergence was obtained during 6 – 8 periods.

The analysis of the numerical model for the new type of the doping profile (Fig.1(b)) gave an unexpected but understandable result. The numerical scheme convergence for this type of the doping profile is very slow. The necessary number of the consequent periods depends on the operating frequency and can change from 30 – 50 for the frequency region 15 – 60 GHz until 150 – 250 periods for 200 – 300 GHz. This very slow convergence is stipulated by the asynchronies movement of the electron and hole avalanches along the same transit time region *v*. It occurs owing to the different drift velocities of the carriers. This type of numerical convergence provokes a large number of the necessary periods and a large computer time.

4 Comparative Analysis

The doping profile structure for the DDR and DAR IMPATT diode active layer is shown in Fig. 1. The accurate analysis for both types of the diodes has been made for the different values of the *p*, *n* and *v* region lengths and for the different donor and acceptor concentrations. The analysis showed that for more or less significant length of the region *v* (more than $0.5\,m$ m) the active properties of the diode are not become. The reason is the same which for the slow mechanism convergence of the numerical model. The electron and hole avalanches have the different transit velocities but they move along the same drift region *v*. It provokes the different time delay for carriers during the transit region movement. The more length of the region *v* gives the more difference in delay time and the active properties are reduced. That is why we need reduce the length of the region *v* to obtain the necessary negative admittance. This is the contrary conclusion to all results of the papers [14-15].

Another positive idea consists of the non symmetric doping profile utilization. This profile gives some compensate of the asynchronies mechanism. Take into account these considerations the non symmetric doping profile diode was analyzed in a wide frequency range. The doping level of the *n*-zone is equal to $0.5\ _{10}17$ cm^{-3}, and for the *p*-zone is equal to $0.2_{10}17$ cm^{-3}. The widths of two these corresponding areas are equal to $0.1\ m$ m and $0.2\ m$ m accordingly. The width of the each *p*-*n* junction was given as $0.02\,m$ m from the technological aspects. The length of the drift zone *v* is equal to $0.32\,m$ m. This type of doping profile provides a concentration of electrical field within the two *p*-*n* junctions.

In Fig. 3 and Fig. 4 the small signal complex admittance i.e. the conductance versus susceptance are presented for the wide frequencies range for DDR and DAR diodes and for the current density J_0 = 30 kA/cm^2.

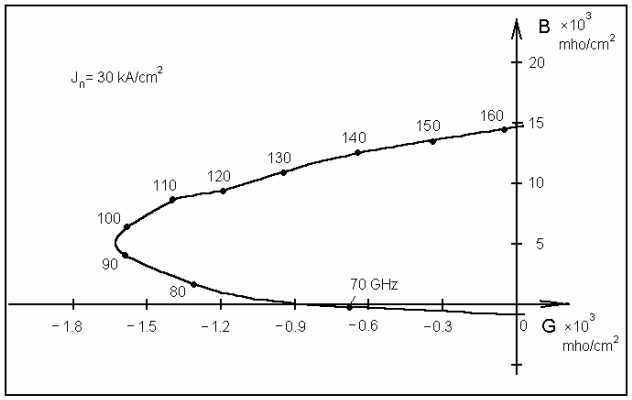

Fig. 3. DDR diode complex small signal admittance (conductance -*G* versus susceptance *B*) plots for different frequencies.

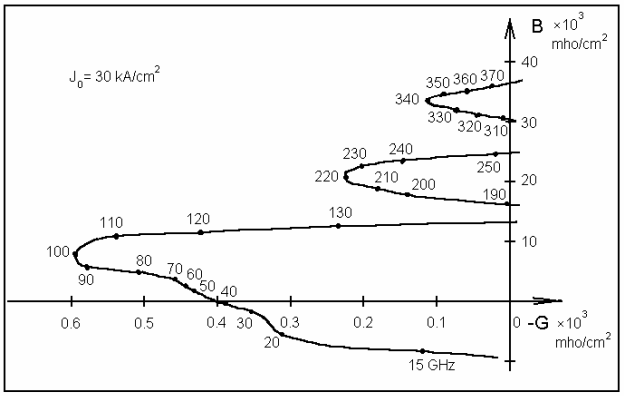

Fig. 4. DAR diode complex small signal admittance (conductance -*G* versus susceptance *B*) plots for different frequencies.

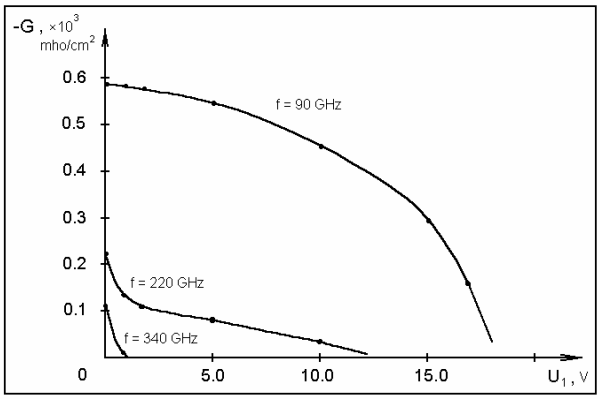

Fig. 5. Conductance *G* dependency as function of first harmonic amplitude U_1 for three frequency zones.

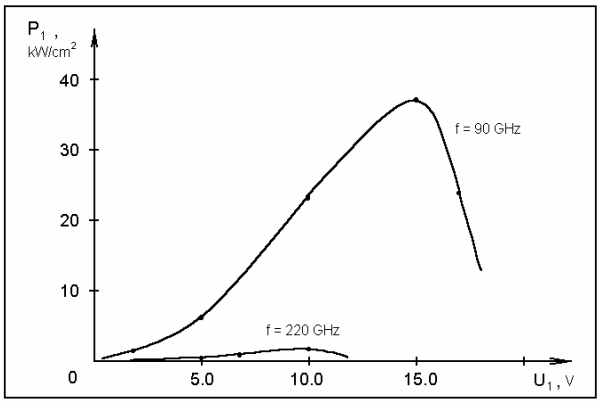

Fig. 6. Generate power *P* as function of first harmonic amplitude U_1 for two frequency zones.

There are some differences of the DAR diode frequency characteristics from the classical DDR IMPATT diodes. First of all the new type of the diode has three active zones in the millimetric range (Fig.4) and the DDR diode has only one zone (Fig.3). The first active zone of the DAR diode is very wide and covers the frequency region from 12 to 138 GHz. The second and the third zones give the perspective to use this structure for the high frequency generation into the millimetric range. The other difference from the usual diodes is the larger value of the real part of the complex admittance -*G* for two more high frequency zones. This effect permits use another frequency zones, at least the second zone, for the microwave power generation. The dependencies of the conductance -*G* as the function of the first harmonic amplitude U_1 are shown in Fig. 5 for three frequency zones and for the same value of the current density J_0 = 30 kA/cm^2. It is clear that the first zone characteristic (f = 90 GHz) has a better behavior. The maximum value of the conductance -*G* is a large and for the small signal achieves near the 600 mho/cm^2. The amplitude dependency for the first zone is a very soft and this provide a significant value of the generate power. Nevertheless the second and third zones (for 220 GHz and for 340 GHz) have the perspective too. These characteristics have a more sharp amplitude dependency and this effect limits the output power. However the possible optimization of the diode internal structure can improve these characteristics and permits to raise the power and the efficiency. The generate power dependencies for two frequency ranges are presented in Fig. 6 as the functions of the first harmonic amplitude. The maximum power density is equal to 37 kW/cm^2 for the first frequency zone (90 GHz) and 1.4 kW/cm^2 for the second one (220 GHz). The last result can serves as the start point for the DAR diode profile optimization to obtain the maximum output power generation for the superior frequency zones.

5 Conclusion

The numerical scheme that has been developed for the analysis of the different types of IMPATT diodes is suitable for the DAR complex doping profile investigation. Some new features of the DAR diode were obtained by the careful analysis on the basis of the precise numerical model. First of all we need to declare that the analysis of the DAR diode is more complicated than DDR because the very slow convergence of the numerical scheme. The principal results were obtained by the precise analysis and contradict the data that had been obtained on the

basis of the approximate models of the DAR diode. These results show that the diode do not have the active properties for the sufficiently large intrinsic region. To obtain the negative conductance we need to reduce the intrinsic region. Nevertheless the diode has a widely first frequency zone generation and the two superior frequency zones with the sufficient output power level. The DAR type of the IMPATT diode can be used for the output power generation in more widely frequency region than well known DDR diode.

Acknowledgment

This work was supported by the Universidad Autónoma de Puebla, under project VIEPIII05G02.

References:

[1] Edited by Kai Chang, *Handbook of Microwave and Optical Components*, John Wile & Sons, N.Y., Vol. 2, 1990.

[2] M. Curow, Proposed GaAs IMPATT Devices Structure for D-band Applications, *Electron. Lett*., Vol. 30, 1994, pp. 1629-1631.

[3] M. Tschernitz and J. Freyer, 140 GHz GaAs Double-Read IMPATT Diodes, *Electron. Letters*, Vol. 31, No. 7, 1995, pp. 582-583.

[4] K.V. Vasilevskii, Calculation of the Dynamic Characteristics of a Silicon Carbide IMPATT Diode, *Sov. Phys. Semicond*., Vol. 26, 1992, pp. 994-999.

[5] R.P. Joshi, S. Pathak and J.A. Mcadoo, Hot-Electron and Thermal Effects on the Dynamic Characteristics of Single-Transit SiC Impact-Ionization Avalanche Transit-Time Diodes, *J. Appl. Phys*., Vol. 78, 1995, pp. 3492-3497.

[6] H.J. Kafka and K. Hess, A Carrier Temperature Model Simulation of a Double-Drift IMPATT Diode, *IEEE Trans. Electron Devices*., Vol. ED-28, No. 7, 1981, pp. 831-834.

[7] A.M. Zemliak and S.A. Zinchenko, Non-linear Analysis of IMPATT Diodes, *Vestnik K.P.I., Radiotechnika*, Vol. 26, 1989, pp. 10-14.

[8] C. Dalle and P.A. Rolland, Drift-Diffusion Versus Energy Model for Millimetric-Wave IMPATT Diodes Modelling, *Int. J. Numer. Modelling*, Vol. 2, 1989, pp. 61-73.

[9] V. Stoiljkovic, M.J. Howes and V. Postoyalko, Nonisothermal Drift-Diffusion Model of Avalanche Diodes, *J. Appl. Phys*., Vol. 72, 1992, pp. 5493-5495.

[10] W.T.Read, A Proposed High-Frequency Negative Resistance Diode, *Bell Syst. Tech. J.*, Vol.37, 1958, pp.401-446.

[11] B. Som, B.B. Pal and S.K. Roy, A Small Signal Analysis of an IMPATT Device having two Avalanche Layers Interspaced by a Drift Layer, *Solid-State Electron*., Vol. 17, 1974, pp. 1029-1038.

[12] D.N. Datta and B.B.Pal, Generalised Small Signal Analysis of a DAR IMPATT Diode, *Solid-State Electron.*, Vol. 25, No. 6, 1982, pp. 435-439.

[13] D.N. Datta, S.P. Pati, J.P. Banerjee, B.B. Pal and S.K. Roy, Computer Analysis of DC Field and Current-Density Profiles of DAR IMPATT Diode, *IEEE Trans. Electron Devices*, Vol. ED-29, No. 11, 1982, pp. 1813-1816.

[14] S.P.Pati, J.P.Banerjee and S.K.Roy, High Frequency Numerical Análisis of Double Avalanche Region IMPATT Diode, *Semicond.. Sci. Technol*. Vol. 6, 1991, pp. 777-783.

[15] A.K. Panda, G.N. Dash and S.P. Pati, Computer-Aided Studies on the Wide-Band Microwave Charactyeristics of a Silicon Double Avalanche Region Diode, *Semicond. Sci. Technol*., Vol. 10, 1995, pp. 854-864.

[16] A. Zemliak, S. Khotiaintsev and C. Celaya, Complex Nonlinear Model for the Pulsed-Mode IMPATT Diode, *Instrumentation and Development*, Vol. 3, No. 8, 1997, pp. 45-52.

[17] A. Zemliak and R. De La Cruz, An Analysis of the Active Layer Optimization of High Power Pulsed IMPATT Diodes, *Computación y Sistemas*, Edición Especial, Diciembre 2002, pp. 99-107.

[18] W.N. Grant, Electron and Hole Ionization Rates in Epitaxial Silicon at High Electric Fields, *Solid-State Electronics*, Vol.16, No.10, 1973, pp.1189-1203.

[19] C. Jacoboni, C. Canali, G. Ottaviani and A. Alberigi Quaranta, A Review of Some Charge Transport Properties of Silicon, *Solid-State Electron*., Vol. 20, 1977, pp. 77-89.

[20] C. Canali, C. Jacoboni, G. Ottaviani and A. Alberigi Quaranta, High Field Diffusion of Electrons in Silicon, *Appl. Phys. Lett.*, Vol. 27, 1975, p. 278.

[21] F. Nava, C. Canali, L. Reggiani, D. Gasquet, J.C. Vaissiere and J.P. Nougier, On Diffusivity of Holes in Silicon, *J. Appl. Phys*., Vol. 50, 1979, p. 922.